Mesoscopic Analysis of Structure and Strength of Dislocation Junctions in fcc Metals

V. B. Shenoy,[1] R. V. Kukta,[2] and R. Phillips[1]
[1]*Division of Engineering, Brown University, Providence, Rhode Island 02912*
[2]*Division of Engineering and Applied Science, California Institute of Technology, Pasadena, California 91125*
(Received 7 July 1999)

We develop a finite-element-based nodal dislocation dynamics model to simulate the structure and strength of dislocation junctions in fcc crystals. The model is based on anisotropic elasticity theory supplemented by the explicit inclusion of the separation of perfect dislocations into partial dislocations bounding a stacking fault. We demonstrate that the model reproduces in precise detail the structure of the Lomer-Cottrell lock already obtained from atomistic simulations. In light of this success, we also examine the strength of junctions culminating in a stress-strength diagram which is the locus of points in stress space corresponding to dissolution of the junction.

PACS numbers: 61.72.Lk, 62.20.Fe

In fcc metals, a key mechanism limiting the movement of dislocations is the "forest intersection" mechanism, where segments of dislocations on a glide plane are rendered immobile as a result of intersection with dislocations on other glide planes. Such intersections can lead to complex *dislocation junction* structures since the cores of the dislocations in these metals are dissociated into partial dislocations separated by a stacking fault [1]. Furthermore, the structure of the junction also depends strongly on the geometric disposition (such as the line directions and Burgers vector) of the participating dislocations. A core level analysis of all the possible junction configurations is therefore important from a number of perspectives. Such core level calculations in conjunction with statistical averaging procedures can possibly provide key parameters that are used in models that predict the mechanical behavior of metallic crystals on a macroscale. These models include single crystal plasticity models [2] and computational models that simulate the dynamics of a large collection of dislocations [3]. In this Letter we develop a mesoscopic dislocation dynamics model that can be used to simulate the structures and strength of dislocation junctions in fcc metals and may obviate the need for direct atomistic simulations of these junctions.

For simple dislocation intersection geometries, the structure of dislocation junctions has been studied extensively using the theory of linear elasticity in a series of classic papers by Hirth and co-workers [4]. Analytical insight into more complicated intersection geometries has been gained by using the line tension approximation for the dislocation lines [5]. While this approach provides a great deal of physical insight into the junction structure and strength, it ignores the extended core structure of the dislocations as well as the long range interaction between the dislocation segments. With rapid advances in computational power in recent years, it has become possible to perform atomistic simulations of dislocation intersections [6–8]. Typically these simulations [7,8] are computationally demanding and raise serious questions concerning the role that boundary conditions play in dictating the results.

In the present study, we develop a mesoscopic method to study the structure and strength of dislocation junctions that includes the dissociation of the dislocation core into partial dislocations. The interaction between the dislocations are treated using the theory of anisotropic elasticity [9]. We find that our method reproduces, in precise detail, all the features of the dislocation junction structure obtained from a full atomistic treatment of the dislocation core. Our results demonstrate that the junction structure is almost entirely determined by elastic interaction between the partial dislocations and the stacking fault energy. In order to clearly demonstrate the role of the stacking fault in determining the junction structure, we consider dislocation junctions in two metals, namely, Al, with a high stacking fault energy ($0.104\ \mathrm{J/m^2}$) and Ag, with a low stacking fault energy ($0.016\ \mathrm{J/m^2}$). We limit our discussions to the Lomer-Cottrell lock [1]; a complete investigation of other junctions will be reported elsewhere.

The simulations are carried out through an adaptive finite element based nodal dislocation dynamics algorithm that is described in detail in Ref. [10]. We start our simulations with straight dislocation lines that are pinned at their end points. Simulations are carried out until the dislocations glide to their equilibrium configuration. Each dislocation line is allowed to split into partial dislocations by accounting for the energy cost of the stacking fault created in the process. A time step of the dynamics process consists of moving the node connecting the segments with a velocity that is proportional to the nodal driving force. The computation of the nodal force requires the knowledge of the force per unit length at certain quadrature points on the dislocation segments that are attached to the node. The force per unit length at any point on a segment consists of a component arising from the stresses due to all the dislocation segments in the system including the segment itself. The Brown regularization procedure is adopted to guarantee that the self-stress contribution is well behaved [10]. When the interaction between the segments belonging to different dislocations is attractive, they approach each other in the process of forming a junction. However,

the stress acting on one of the segments due to the other one diverges as their separation vanishes. To remove this difficulty, we treat the stresses as constant for distances less than a critical separation distance, r_c, with a value equal to that of the stress computed at r_c. As a result, the segments are locked once they are closer than this critical distance; a junction has formed. From an elastic perspective, at distances larger than r_c, the stresses produced by the junction segments correspond to those produced by a dislocation whose Burgers vector is the vector sum of those of the two segments that make up the junction. Once the junction is formed, it can unzip if the external stresses cause the segments that form the junction to move away from each other. The calculations described here were carried out with $r_c = b$, although we have also considered the cases in which the cutoff was $b/2$ and $2b$, without noticeable change to the resulting junction structures. In addition to the stress from the dislocation segments, the force per unit length consists of a component arising from the stacking fault. This component is normal to the dislocation segment and has a magnitude that equals the stacking fault energy and acts in a direction tending to shrink the stacking fault. In the simulations that we describe, we have ignored the frictional stress since we have found that its inclusion is unimportant. A key feature of our simulations is the adaptive positioning of the nodes, so that regions with large curvature have more nodes per unit length.

We demonstrate our results by first considering the equilibrium configuration of a Lomer-Cottrell lock as shown in Fig. 1. This configuration has been chosen so as to make a direct comparison of our results with the atomistic simulations for Al reported in Ref. [8]. The pinning points are arranged such that in the starting configuration the dislocation line directions make an angle of 60° with the $[\bar{1}, 1, 0]$ direction. This direction coincides with the line of intersection of the slip planes of the dislocations that form the junction. The line directions of each of the partial dislocations and their slip plane normals are given in the figure. We follow the notation described in Ref. [1] to label the Burgers vectors of the partial dislocations by referring to the Thompson tetrahedron. For example, the $(a/2)[0, 1, \bar{1}](111)$ dislocation splits into partial dislocations $A\delta$ and δC with Burgers vectors $(a/6)[\bar{1}, 2, \bar{1}]$ and $(a/6)[1, 1, \bar{2}]$, respectively. As is evident from the figure, the junction segment in the case of Al has split into separate parts. A stair-rod segment with Burgers vector $\gamma\delta$ of the type $(a/6)\langle 110\rangle$ forms an extended node on the left side of the junction. The remaining part of the junction is a sessile Lomer dislocation segment. The length of the stair-rod segment is 38 Å, while the Lomer is 42 Å, which is in excellent agreement with the atomistic results [8]. The dislocation dynamics model also agrees with the atomistic results in predicting the structure of the right hand node, which is pointlike and is the meeting point of constricted dislocation segments.

As an extension of earlier results and to highlight the dependence of the junction structure on the stacking fault

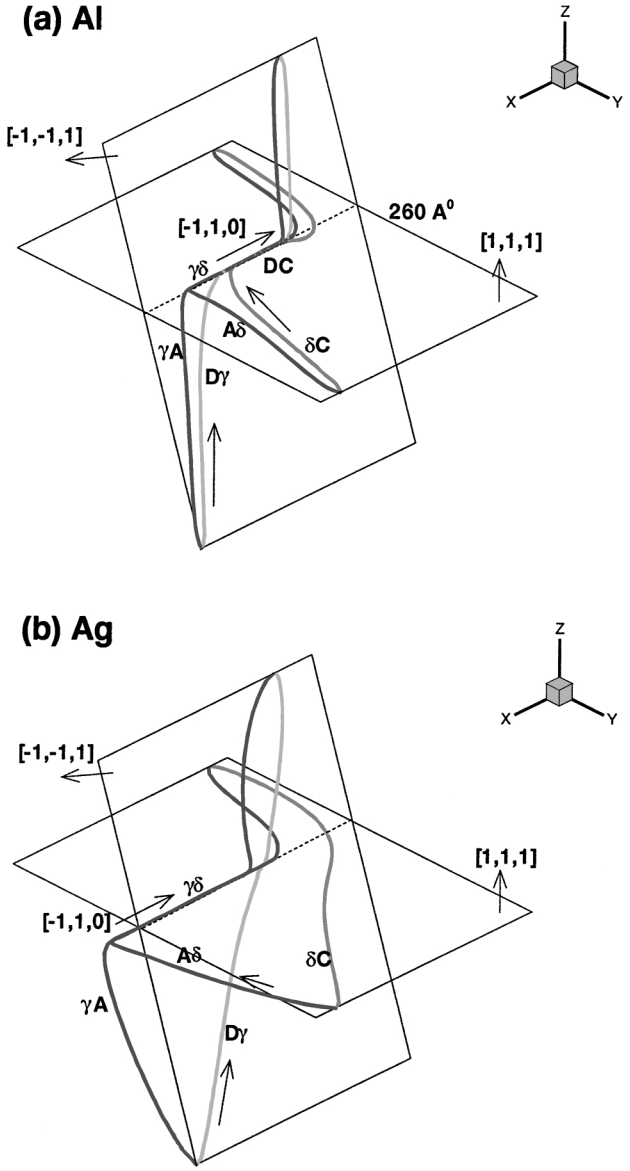

FIG. 1. Structure of the Lomer-Cottrell junction in Al and Ag. The line directions and the Burgers vectors of the dislocation segments are indicated in the figure. The junction forms along the dotted line, which is the line of intersection of the two slip planes.

energy, we have also computed the geometry of the Lomer-Cottrell junction in Ag. The dislocation junction in Ag, for this configuration, has an entirely different structure. The junction segment is entirely composed of a stair-rod dislocation of length 180 Å The smaller stacking fault energy keeps the segments δC and $D\gamma$ from participating in the junction formation process.

We now consider the effect of altering the junction angle on the structure of the dislocation junction. We use ϕ to denote the angle between the dislocation line direction in the starting configuration and the $[\bar{1}, 1, 0]$ direction, l_J for the junction length, and $2l$ for the distance between the pinning points. In Fig. 2, we plot the junction length and structure as the orientation of the pinning points

is altered. For comparison we also show the results obtained by using both the isotropic [5] and anisotropic line-tension models within isotropic elasticity. We find that the results of our simulations are in very good agreement with the predictions of the anisotropic line-tension model [11]. For the positive angle junctions, the participating dislocations enter in mostly "edge" orientation, while in the case of negative angle junctions, they enter in the screw orientation. As a result, the energy gain in the former case is bigger than the latter by a factor $1/(1-\nu)$, where ν is the Poisson ratio. This has two immediate consequences that are borne out by our simulations: first, the edgelike junctions are stabler to higher incidence angles, and, second, the edge locks are strong relative to "screw" locks for the same incidence angle. In fact, transmission electron microscopy studies of dislocation junctions [12] reveal a preponderance of the edgelike junctions over their screw counterparts. While one explanation for the instability of the screw junctions is the ability of the parent dislocations to cross-slip resulting in the transformation of the sessile lock to a glissile one, our simulations provide yet another explanation for the stability of the edgelike junctions.

Far more interesting than the structure of junctions is their behavior under stress. Figure 3 shows the evolution of the dislocation junction in Fig. 1a under the influence of an externally applied stress. The resolved shear stress on the dislocations in the $(1,1,1)$ and $(\bar{1},\bar{1},1)$ slip planes are labeled σ_1 and σ_2, respectively. We have chosen the orientation of the applied stress for this series of pictures such that $\sigma_1 = \sigma_2$. On increasing the stress, the length of the Lomer segment initially increases on going from no applied stress to a stress of 0.006μ (μ is the shear modulus). On increasing the stress further, the junction translates and undergoes an unzipping mechanism, whereby the length of the Lomer segment decreases. This behavior is evident for the stress level of 0.009μ. The junction breaks at a stress level of about 0.012μ after which they continue to bow out. The configuration shown at stress of 0.012μ, is not in equilibrium, but a snapshot after the junction has been destroyed. We have carried out similar calculations for several values of resolved shear stress acting on the two dislocations. A "yield surface" for dislocation destruction is shown in Fig. 4. This surface is symmetric about the line $\sigma_1 = \sigma_2$ but depends on the sign of σ_1 and σ_2. This symmetry breaking is readily understood by looking at the configurations of the dislocations under action of positive and negative σ_1 (denoted in Fig. 4 by points A and B, respectively) with $\sigma_2 = 0$. The presence of the stair-rod node makes it more difficult for the horizontal segment to bow out in case (A) compared to case (B) and requires a larger value of shear stress to break the junction.

It is interesting to compare the predictions of the line-tension model and the atomistic simulations with the results obtained from our simulations. An important prediction of the line-tension model is the scaling of the breaking stress of symmetric junctions with the distance

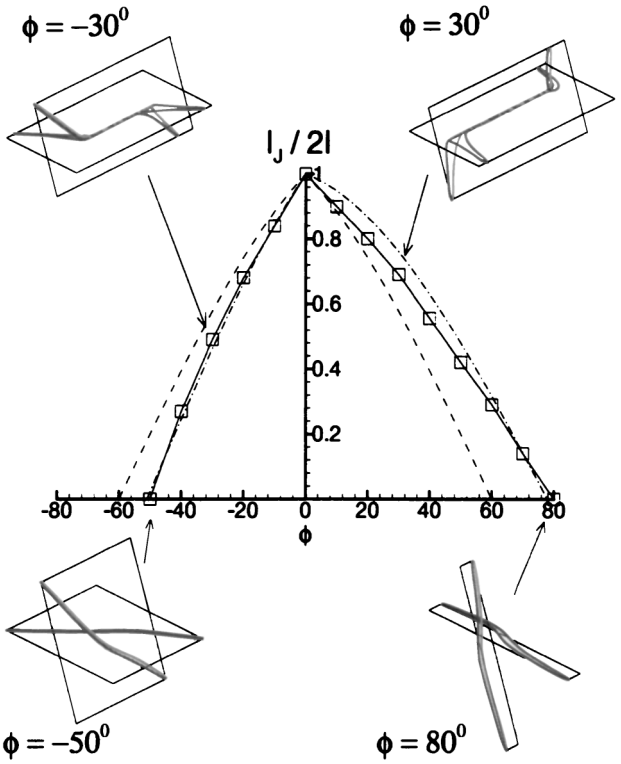

FIG. 2. Junction length of the Lomer-Cottrell lock in Al as a function of the line directions of the participating dislocations. The dashed and dash-dotted lines are the predictions of the direction dependent and independent line-tension models, respectively, and the "squares" are the results obtained using our mesoscopic model. We also show the evolution of the junction structure as the line directions are varied.

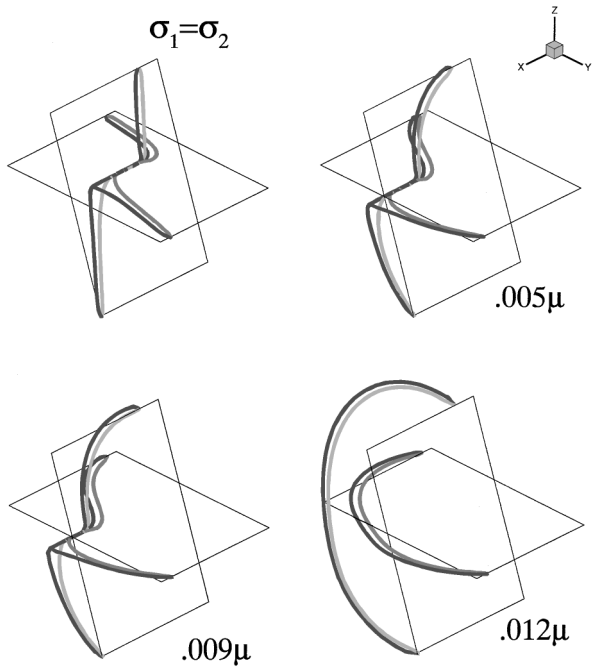

FIG. 3. Evolution of the symmetric Lomer-Cottrell lock in Fig. 1a, on applying an external stress. The resolved shear stress on the two junctions is the same.

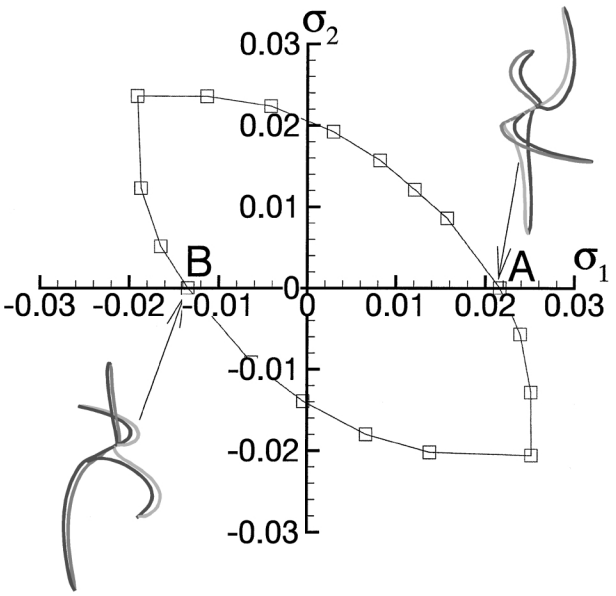

FIG. 4. The yield surface for the symmetric Lomer-Cottrell lock in Fig. 1a. The stresses are in the units of shear modulus of Al. We also display the structure of the junctions prior to destruction for the points marked *A* and *B*.

between the pinning points, written as $2l$. The line-tension model predicts the average critical resolved shear stress to break the symmetric junctions to be $\approx 0.5\mu b/l$. We have simulated the breaking of symmetric junctions with lengths ranging from 300 Å to 1 μm by applying the external stress in different orientations. We have found that the critical breaking stress scales as $\sigma_c \sim \mu b/l$. For the cases $\sigma_1 = \sigma_2$ and $\sigma_1 = -\sigma_2$ the critical resolved shear stress behaves like $\sigma_c = 0.64\mu b/l$ and $\sigma_c = 1.24\mu b/l$, respectively. For the 300 Å junction, for the case when $\sigma_1 = 1.3\sigma_2$, the atomistic simulations gave $\sigma_c = 0.017\mu = 0.8\mu b/l$, which is in good agreement with our results.

Before presenting our concluding remarks, we point out the features that are missed in our model and the effect they may have on the results discussed thus far. In our simulations, the dislocations do not acquire a jog as they cross. While this does not affect the junction structure, it will alter the breaking stress, since the external stress should supply the energy required to create the jog. However, the jog contribution to the breaking stress is only a small fraction of the stress required to unzip the junctions [5]. In order to examine the effect of the stress cutoff distance, r_c, we have also carried out all the above simulations by choosing r_c to equal $b/2$ and $2b$. The junction structure showed very little difference in the two calculations. Also, the breaking stress in all the cases was within 10% of the values reported here.

In conclusion, we have developed an efficient method to study dislocation interactions in fcc metals. We have illustrated that the method can provide "rules" like critical angle for junction formation and breaking stress criteria, which can be used in 3D dislocation dynamics models. The results from our simulations for junctions in different configurations, when appropriately averaged, can provide parameters related to junction strength in models for single crystal plasticity. Fits to these parameters from tension tests on single crystals have revealed a hierarchy of junction strengths in fcc crystals [13]. Work is in progress to verify the observed hierarchy on the basis of our simulations.

We are grateful to V. Bulatov, M. Fivel, L. Kubin, A. Needleman, M. Ortiz, D. Rodney, and G. Saada for illuminating discussions. We appreciate the support of the Caltech ASCI and the Brown MRSEC Programs. We also acknowledge the computational resources of Brown University's Technology Center for Advanced Scientific Computing and Visualization.

[1] See, for example, J. P. Hirth and J. Lothe, *Theory of Dislocations* (Kreiger, Malabar, FL, 1992).
[2] J. L. Bassani, Adv. Appl. Mech. **30**, 191 (1994).
[3] M. Verdier, M. Fivel, and I. Groma, Model. Simul. Mater. Sci. Eng. **6**, 755 (1998), and references therein.
[4] J. P. Hirth, J. Appl. Phys. **32**, 700 (1961); **33**, 2286 (1962); T. Jossang, J. P. Hirth, and C. S. Hartley, *ibid.* **36**, 2400 (1965).
[5] G. Saada, Acta Metall. **8**, 841 (1960); G. Schoeck and R. Frydnam, Phys. Status Solidi **53**, 661 (1972).
[6] V. Bulatov, F. Abraham, L. Kubin, B. Devincre, and S. Yip, Nature (London) **391**, 669 (1998).
[7] S. J. Zhou, D. L. Preston, P. S. Lomdahl, and D. M. Beazley, Science **279**, 1525 (1998).
[8] D. Rodney and R. Phillips, Phys. Rev. Lett. **82**, 1704 (1999).
[9] D. J. Bacon, D. M. Barnett, and R. O. Scattergood, Prog. Mater. Sci. **23**, 51 (1979).
[10] M. S. Duesbery, N. P. Louat, and K. Sadananda, Philos. Mag. A **65**, 311 (1995); K. W. Schwarz, J. Appl. Phys. **85**, 108 (1999); R. V. Kukta, Ph.D. thesis, Brown University, 1998.
[11] Also see L. K. Wickham, K. W. Schwarz, and J. S. Stolken, Phys. Rev. Lett. **83**, 4574 (1999).
[12] H. P. Karnthaler, Philos. Mag. A **38**, 141 (1978); A. Korner and H. P. Karnthaler, Philos. Mag. A **44**, 275 (1981).
[13] See, for example, P. Franciosi and A. Zaoui, Acta Metall. **30**, 1627 (1982).